5698 *Macromolecules* **1997,** *30,* 5698−5703

# Lamellar Domain Spacings of Diblock Copolymer/Homopolymer Blends and Conformations of Block Chains in Their Microdomains

**Naoya Torikai, Naomi Takabayashi,[1] and Ichiro Noda**

*Department of Applied Chemistry, Graduate School of Engineering, Nagoya University,*
*Furo-cho, Chikusa-ku, Nagoya 464-01, Japan*

**Satoshi Koizumi and Yukio Morii**

*Neutron Scattering Laboratory, Japan Atomic Energy Research Institute, Tokai,*
*Naka-gun, Ibaraki 319-11, Japan*

**Yushu Matsushita***

*Neutron Scattering Laboratory, The Institute for Solid State Physics,*
*The University of Tokyo, Tokai, Naka-gun, Ibaraki 319-11, Japan*

*Received December 31, 1996; Revised Manuscript Received June 26, 1997*[⊗]

ABSTRACT: Lamellar domain spacings (*D*) of blends of a styrene-2-vinylpyridine (SP) diblock copolymer and homopolymers corresponding to the block polymers (S and/or P), of which molecular weights are lower than that of the block polymer, were examined by small-angle X-ray scattering (SAXS), and the dimensions of block chains in the lamellae were investigated by small-angle neutron scattering (SANS). The *D*'s for SP/S/P ternary and SP/S (or SP/P) binary blends increase with increasing the molecular weight of the homopolymers, $M_H$, as well as the volume fraction of the homopolymers, $\Phi_H$, in the corresponding lamella. The variations of the *D*'s with $\Phi_H$ for the blends with homopolymers having different $M_H$'s reveal that homopolymers with higher $M_H$ are localized at the center of the corresponding lamella, while those with lower $M_H$ are distributed throughout the lamella. Moreover, the comparison between the *D*'s for ternary and binary blends with homopolymers having equal $M_H$'s implies that the homopolymers in binary blends are more localized than those in ternary blends. In these ternary and binary blends the radii of gyration of styrene block chains along the direction parallel to lamellar interface are not much different from that for a pure diblock copolymer irrespective of $\Phi_H$ as well as $M_H$.

## Introduction

The blends of an AB diblock copolymer and homopolymers corresponding to the block polymers (A and/or B) show complicated phase diagrams due to the coexistence of micro- and macrophase separations.[2−5] These phase separation behaviors depend not only on the volume fraction of the homopolymer, $\Phi_H$, in the blends but also on the molecular weight of the homopolymer, $M_H$. When $M_H$ is lower than that of the corresponding block chain, $M_B$, the microphase separation region covers a wide range on the phase diagram, while the macrophase separation region appears dominantly when $M_H$ is higher than $M_B$.

The morphological studies of diblock copolymer/homopolymer blends have been mainly focused on the microphase separation region on their phase diagrams so far,[6−10] though some interesting morphologies formed by macrophase separation were studied recently.[11,12] Hashimoto et al.[6,7] and Winey et al.[8−10] studied the morphologies of AB/A (or AB/B) binary blends with homopolymers having various molecular weights and found that morphological transitions occur from the initial microdomain structures of pure AB diblock copolymers to new more stable ones when $M_H$'s are sufficiently lower than $M_B$, while no morphological transitions occur when $M_H$'s are comparable to $M_B$. They also examined the increments of domain spacings by small-angle X-ray scattering (SAXS) to clarify the homopolymer distributions in those binary blends;[6,7,13] homopolymers with considerably low $M_H$ are uniformly dissolved in the corresponding microdomain, while those with $M_H$ comparable to $M_B$ are localized at the center of the microdomain. These results are qualitatively consistent with the distribution profiles of homopolymers in lamellar microdomains for binary blends evaluated by neutron reflectivity measurements.[14] It was concluded from these results that microdomains are extended by uniform solubilization of the homopolymers with considerably low $M_H$, and the extension of either one of two microdomains along the interface leaving the other one unchanged is the driving force of the morphological transitions observed in the binary blends. On the other hand, AB/A/B ternary blends, in which equal amounts of A and B homopolymers having equal $M_H$'s are mixed with an AB diblock copolymer, did not reveal morphological transitions even though $M_H$'s were sufficiently lower than $M_B$.[6]

In a previous work[15] we studied the chain conformations of three homopolymers, of which molecular weight ratios to that of the block polymer, $M_H/M_B$, are 0.5, 1, and 2, in lamellar microdomains for binary blends by small-angle neutron scattering (SANS), and found that the radii of gyration of those homopolymers are almost equal to unperturbed dimensions at least along the direction parallel to lamellar interface. Thus, it is worthwhile to clarify both homopolymer distributions and the chain conformations of block chains as well as homopolymers focusing on the difference in ternary and binary blends for the understanding of phase-separated structures formed by diblock copolymer/homopolymer blends at the molecular level.

In this work we compared homopolymer distributions in AB/A/B ternary and AB/A (or AB/B) binary blends,

---

[⊗] Abstract published in *Advance ACS Abstracts,* August 15, 1997.

S0024-9297(96)01936-5 CCC: $14.00

**Table 1. Molecular Characteristics of Diblock Copolymers**

| sample code | $M_\mathrm{n} \times 10^{-3}$ [a] | $M_\mathrm{w}/M_\mathrm{n}$ [b] | $\Phi_\mathrm{S}$[c] |
|---|---|---|---|
| SP-77 | 77−72 | 1.02 | 0.53 |
| SP-43 | 72−84 | 1.02 | 0.51 |
| DP-77 | 92−75 | 1.09 | 0.50 |

[a] $M_\mathrm{n}$ is the number-averaged molecular weight determined by membrane osmometry. [b] Determined by GPC chromatograms. [c] $\Phi_\mathrm{S}$'s are the volume fractions of styrene block chains determined by elemental analysis.

**Table 2. Molecular Characteristics of Homopolymers**

| sample code | $M_\mathrm{n} \times 10^{-3}$ | $M_\mathrm{w}/M_\mathrm{n}$ | $M_\mathrm{H}/M_\mathrm{B}$[b] |
|---|---|---|---|
| RMS-7 | 3.7[a] | 1.02 | 0.05 |
| VPK-19 | 6.9[a] | 1.30 | 0.08 |
| RMS-3 | 13 | 1.08 | 0.17 |
| VPK-17 | 16 | 1.16 | 0.22 |
| RMS-4 | 30 | 1.02 | 0.38 |
| VPK-14 | 29 | 1.02 | 0.40 |
| RMS-5 | 61 | 1.02 | 0.78 |
| VPK-18 | 57 | 1.02 | 0.79 |

[a] These molecular weights were determined by GPC chromatograms using calibration curves from polystyrenes and poly(2-vinylpyridine)s. [b] $M_\mathrm{H}/M_\mathrm{B}$ is the ratio of the molecular weight of homopolymer ($M_\mathrm{H}$) to that of the corresponding block chain ($M_\mathrm{B}$).

where A and B are polystyrene (PS) and poly(2-vinylpyridine) (P2VP), respectively, by measuring the increments of lamellar domain spacings by SAXS. We also investigated the chain conformations of block chains in lamellar microdomains for these blends by SANS and compared them directly. Although the chain conformations of block chains in ternary blends with the homopolymer having considerably low $M_\mathrm{H}$ were previously studied by SANS,[16] the contrast-matching method adopted in that study was not appropriate for observing the single-chain scattering of block chains. Thus, all the blend specimens used in this work were prepared according to the contrast-matching method proposed by Quan et al.,[17] i.e., composition-matched PS−P2VP diblock copolymers and phase-matched PS's were prepared for SANS measurements.

## Experimental Section

Samples used in this study are two styrene-$h_8$−2-vinylpyridine (SP) diblock copolymers, one styrene-$d_8$−2-vinylpyridine (DP) diblock copolymer, and four pairs of poly(styrene-$d_8$−*ran*-styrene-$h_8$)s (RMS) and P2VP's (VPK). The RMS's are phase-matched polystyrenes, of which weight fractions of styrene-$d_8$ segment were designed to be 0.11 so as to equalize their coherent scattering length densities to that of P2VP. All the samples were prepared by anionic polymerization using cumylpotassium as an initiator in tetrahydrofuran (THF) at −78 °C. The detailed procedures of the polymerizations were reported previously.[15,18] Molecular characteristics of the diblock copolymers and the homopolymers are listed in Tables 1 and 2, respectively. As shown in Table 1, two SP and one DP diblock copolymers, used for preparation of composition-matched diblock copolymer blends, have almost the same molecular characteristics, i.e., the same chain lengths and the same compositions, to one another except for deuterium-labeling of styrene block chain.[19] Each pair of homopolymers, RMS and VPK, has almost the same molecular weight, and their molecular weights, $M_\mathrm{H}$, are all lower than that of the corresponding block chain, $M_\mathrm{B}$, as shown in Table 2. The weight fractions of styrene-$d_8$ segment of all the RMS's used were determined to be 0.11 by pyrolysis-gas chromatography-mass spectrometry (PyGC-MS).

The composition-matched diblock copolymers, abbreviated as CMB hereafter, were prepared by mixing DP-77 and SP-77 or SP-43 at the ratios of 0.11/0.89 by weight and were used as parent diblock copolymers for all diblock copolymer/homopolymer blends. In this study two kinds of blends, i.e., CMB/RMS/VPK ternary blends and CMB/RMS or CMB/VPK binary blends, were prepared. In the ternary blends, corresponding pairs of RMS and VPK in Table 2 were added in equal amounts, so that these blends exhibit lamellar structures irrespective of the volume fraction of homopolymer, $\Phi_\mathrm{H}$, in the corresponding microdomain since their parent diblock copolymers have lamellar structures, while in the binary blends, $\Phi_\mathrm{H}$ of either RMS or VPK was limited to be lower than 0.45 to maintain lamellar structures. Film specimens for scattering measurements were prepared by solvent-casting from 5 wt % THF solutions of the blended polymers so as to be about 0.15 mm thick, and followed by annealing at 150 °C in vacuum for a week.

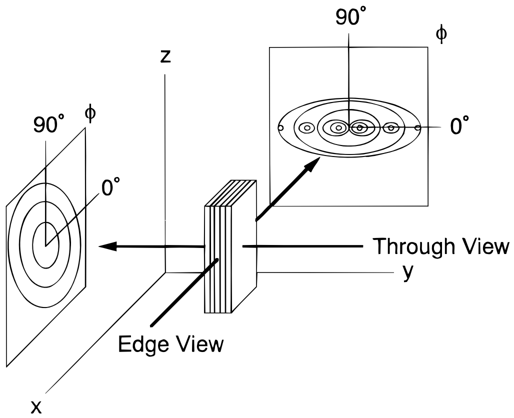

**Figure 1.** Geometrical relationship among an irradiated beam, a film specimen, and a two-dimensional position-sensitive detector in SANS measurements. SAXS intensities were measured by scanning a scintillation counter along the direction of 0° in azimuthal angle, $\phi$.

SAXS measurements were performed with a Kratky U-slit camera of Anton Paar Co. equipped with a step scanner and a scintillation counter. The details of SAXS experimental conditions were reported previously.[20] SAXS intensities were measured at the edge view, in which an X-ray beam is irradiated along the direction parallel to film surface as shown in Figure 1, since lamellar structures are preferentially oriented along the direction parallel to the solvent-cast film surfaces. SANS measurements were performed on the SANS-J spectrometer at the JRR-3M research reactor of Japan Atomic Energy Research Institute (JAERI). The distance between a sample and a two-dimensional position-sensitive detector was 8 m. The wavelength, $\lambda$, of neutrons used was 0.6 nm, and its distribution, $\Delta\lambda/\lambda$, is designed to be 13%. SANS intensities were measured mainly at the through view, in which a neutron beam is irradiated along the direction perpendicular to film surface as shown in Figure 1. For a few specimens the edge view measurements were performed to check contrast-matching. These SANS intensities were corrected for background and incoherent scattering intensities.

## Results

Figure 2a shows SAXS profiles of ternary blends with homopolymers, i.e., RMS and VPK, having various molecular weights at 0.5 for $\Phi_\mathrm{H}$, along with that of their parent CMB (DP-77/SP-77), where $q$ is the magnitude of the scattering vector defined as $(4\pi/\lambda)\sin\theta$ and $2\theta$ is the scattering angle. These profiles exhibit strong diffraction peaks at the positions of $q_n = nq_1$, where $n$ is the integer and $q_n$ is the magnitude of scattering vector at the $n$th order peak, indicating that lamellar structures are formed. The disappearance of the even-order peaks can be attributed to the structure factors of lamellar structures,[20] indicating that the thicknesses of PS and P2VP lamellae are almost equal to each other. Moreover, the positions of all the odd-order peaks are

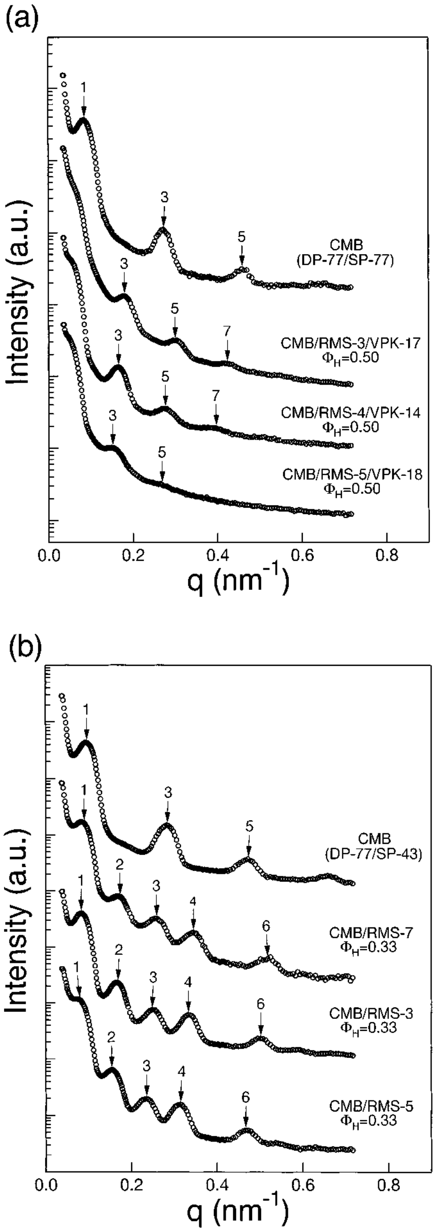

**Figure 2.** (a) SAXS profiles of a parent composition-matched diblock copolymer (CMB; DP-77/SP-77) and its ternary blends with homopolymers, i.e., RMS's and VPK's, having various molecular weights at 0.50 for the volume fractions of homopolymers, $\Phi_H$, in the corresponding microdomain. (b) SAXS profiles of a parent diblock copolymer (CMB; DP-77/SP-43) and its binary blends with RMS's at 0.33 for $\Phi_H$.

shifted toward the low $q$ region with increasing $M_H$. Similar results were obtained for ternary blends at different $\Phi_H$'s from 0.50, though their SAXS profiles are not shown here. Figure 2b shows SAXS profiles of a parent CMB (DP-77/SP-43) and its binary blends with RMS's having various molecular weights at 0.33 for $\Phi_H$. These profiles also exhibit diffraction peaks at the $q$-values of integer-order, though the fifth-order peaks disappear owing to the structure factors. These facts imply that the PS:P2VP lamellar thickness ratios are about 3:2, which were obtained by mixing RMS's about 33% by volume in PS lamellae. The peak-positions are obviously shifted to the low $q$ region with increasing $M_H$, though their shifts are smaller than those of ternary blends at the same $\Phi_H$. Similar results were obtained for binary blends with RMS's at different $\Phi_H$'s from 0.33 and the blends with VPK's except the facts that different order peaks disappear owing to different structure factors, though their SAXS profiles are not shown here.

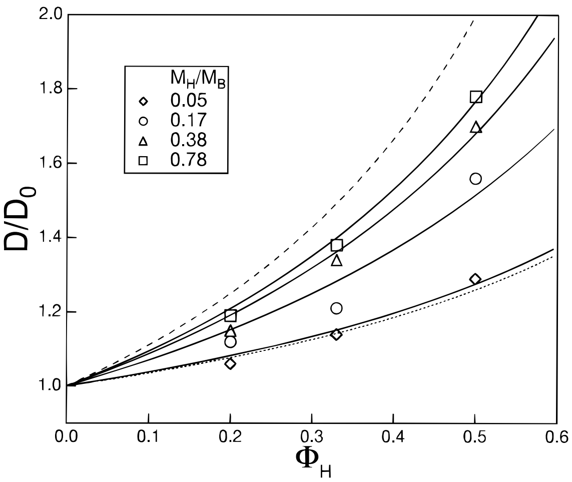

**Figure 3.** Lamellar domain spacings, $D$, for ternary blends normalized to that of a pure diblock copolymer, $D_0$, as a function of $\Phi_H$. $D_0$ values for two parent diblock copolymers, i.e., DP-77/SP-77 and DP-77/SP-43, are 67.0 and 67.3 nm, respectively. Diamonds, circles, triangles, and squares denote the data for the blends with the homopolymers, of which $M_H/M_B$ ratios are 0.05, 0.17, 0.38, and 0.78, respectively. The broken and dotted lines are calculated from eqs 4 and 7, respectively, and the solid lines are the least-squares fits of eq 10 to the data.

Lamellar domain spacings, $D$, were evaluated according to the Bragg's condition, $D = 2\pi n/q_n$. The domain spacings for two parent diblock copolymers, i.e., DP-77/SP-77 and DP-77/SP-43, $D_0$'s, were evaluated to be 67.0 and 67.3 nm, respectively. Thus, $D$ values evaluated for ternary blends were normalized to $D_0$ and were plotted against $\Phi_H$ in Figure 3. This figure indicates that $D/D_0$ values are all higher than unity and increase with increasing $M_H$ as well as $\Phi_H$. Parts a and b of Figure 4 show the plots of $D/D_0$ against $\Phi_H$ for binary blends of CMB/RMS and those of CMB/VPK, respectively. These $D/D_0$ values increase with increasing $M_H$ and $\Phi_H$, though the dependences are somewhat different from those of ternary blends.

In SANS profiles of blend specimens at the edge view, distinct diffraction peaks from lamellar structure were observed, though the profiles are not shown here. Since it is difficult to distinguish the single-chain scattering of block chains from these profiles, the radii of gyration of block chains along the direction perpendicular to lamellar interface, i.e., $y$-direction in the coordinates shown in Figure 1, could not be evaluated. The reasons for this unexpected appearance of diffraction peaks at matching conditions for scattering length densities between PS and P2VP lamellae were fully discussed in our previous works.[15,21] The degrees of lamellar orientation for blend specimens were evaluated from SANS diffraction patterns at the edge views as $<\cos^2 \phi>^{1/2}$, where $\phi$ is the azimuthal angle on the two-dimensional detector defined in Figure 1, and they were confirmed to be almost the same as those for pure diblock copolymers.[22] At the through view, on the other hand, the diffraction peaks were not observed for most of blend specimens as shown in Figure 5a. SANS profiles without the diffraction peaks can be assumed to consist of only the single-chain scattering from block chains. Thus, these scattering intensities at the through view are related to the radius of gyration of block chain along the direction parallel to lamellar interface, $R_{g,k}$, where $k$ is $x$ or $z$ in the coordinates shown in Figure 1,

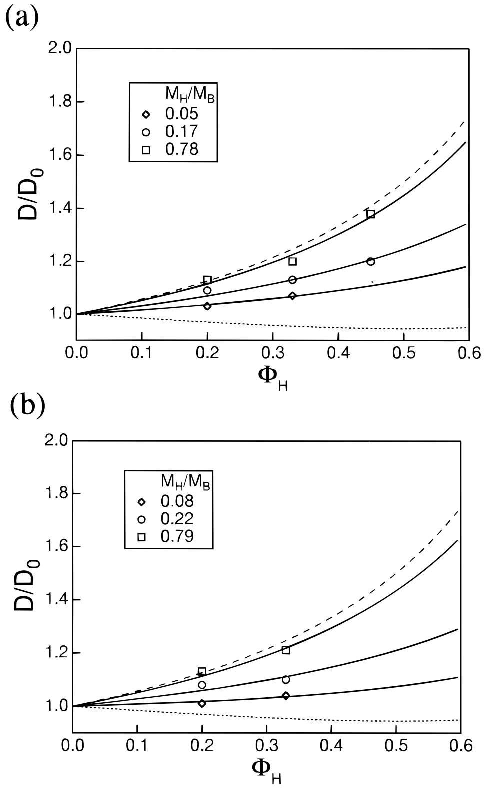

**Figure 4.** $D/D_0$'s for binary blends with (a) RMS's and (b) VPK's as a function of $\Phi_H$. Symbols are the same as in Figure 3. The broken and dotted lines are calculated from eqs 5 and 8, respectively, and the solid lines are the least-squares fits of eq 11 to the data.

according to the Guinier's approximation

$$I(q) = I(0)\exp(-q^2 R_{g,k}{}^2)\ (k = x \text{ or } z) \tag{1}$$

The value of $R_{g,k}$ ($k = x$ or $z$) was evaluated from the slope of the Guinier plots of the scattering intensities as shown in Figure 5b, where the upper limit of the Guinier range defined as $q^2R_{g,k}{}^2 < 1.3^2/3$ was indicated by the vertical broken line. Hereafter, the radius of gyration of a block chain evaluated at the through view is represented by $R_{g,x}$, for simplicity, though $x$- and $z$-axes are equivalent as shown in Figure 1.

The values of $R_{g,x}$ for two parent diblock copolymers, DP-77/SP-77 and DP-77/SP-43, were evaluated to be $3.7_4 \pm 0.12$ and $3.8_4 \pm 0.23$ nm, respectively. These values are consistent with those, 3.7 and 3.6 nm, evaluated from the following empirical equation[22] by using the number-averaged molecular weight of styrene block chains reduced to poly(styrene-$h_8$), i.e., $7.8 \times 10^4$ for DP-77/SP-77 and $7.3 \times 10^4$ for DP-77/SP-43, respectively

$$R_{g,x} = 0.028_9 M^{0.43\pm0.03}\ (\text{nm}) \tag{2}$$

$R_{g,x}$'s normalized to that for their parent diblock copolymers, $R_{g,xp}$, for ternary and binary blends are plotted against $\Phi_H$ in Figures 6 and 7, respectively. The values of $R_{g,x}/R_{g,xp}$ ($\equiv \gamma_x$) appear slightly higher but close to unity irrespective of $M_H$ as well as $\Phi_H$, taking account of experimental errors.

## Discussion

If all the homopolymers dissolved in the corresponding lamella are localized perfectly at the center of the lamella without changing the chain conformations of block polymers and the distances between the neighboring chemical junctions connecting PS and P2VP block chains at lamellar interface, the lamella will be extended only along the direction normal to lamellar interface. When the volume fraction of i-block chain (i = PS or P2VP) in a diblock copolymer is 0.5, which is practically applicable to the present sample, the thickness of the lamella, $D_i$, extended is given by the

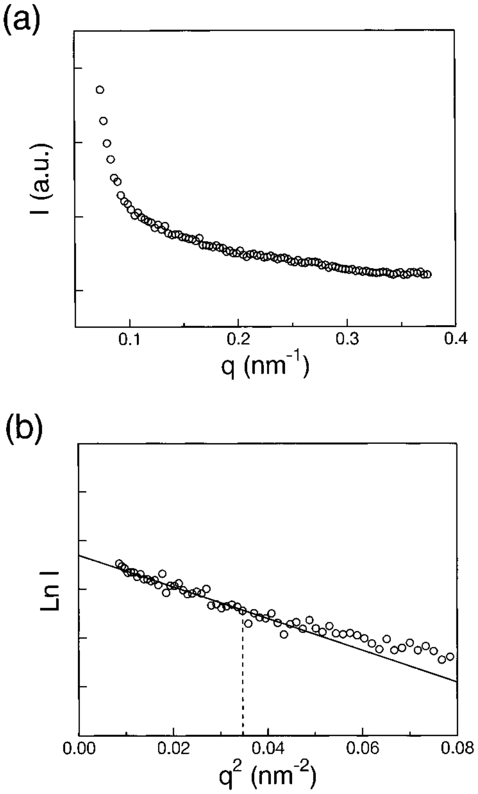

**Figure 5.** (a) SANS intensities at the through view. Sample: a ternary blend with RMS-5 and VPK-18, of which $M_H/M_B$ is 0.78, at 0.33 for $\Phi_H$. (b) Guinier plots of the scattering intensities shown in Figure 5a. The vertical broken line indicates the upper limit of the Guinier range. The radius of gyration of block chain along the direction parallel to lamellar interface, $R_{g,x}$, evaluated from this figure is $4.0_6 \pm 0.15$ nm.

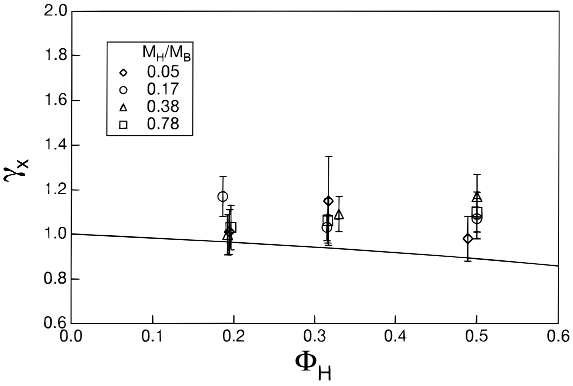

**Figure 6.** Ratios, $\gamma_x$'s, of radii of gyration, $R_{g,x}$'s, of styrene block chains to that for a pure diblock copolymer, $R_{g,xp}$, for ternary blends with homopolymers having various molecular weights as a function of $\Phi_H$. $R_{g,xp}$ values for two parent diblock copolymers, i.e., DP-77/SP-77 and DP-77/SP-43, are $3.7_4 \pm 0.12$ and $3.8_4 \pm 0.23$ nm, respectively. Symbols are the same as in Figure 3 and a solid line denotes the values calculated from eq 12.

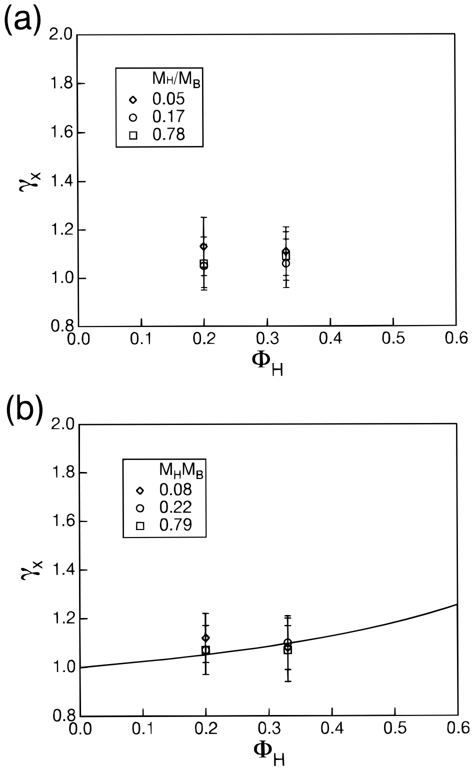

**Figure 7.** Values of $\gamma_x$ of styrene block chains for binary blends with (a) RMS's and (b) VPK's as a function of $\Phi_H$. Symbols are the same as in Figure 4. The solid line in part b denotes the values calculated from eq 13.

following equation

$$D_i = D_0/[2(1 - \Phi_H)] \tag{3}$$

where $D_0$ is the lamellar domain spacing for a pure diblock copolymer. From eq 3, lamellar domain spacing, $D$ $(=D_{PS} + D_{P2VP})$, for a ternary blend can be derived as

$$D = D_0/(1 - \Phi_H) \tag{4}$$

when equal amounts of homopolymers are mixed in both PS and P2VP phases, while $D$ can be expressed by

$$D = D_0(2 - \Phi_H)/[2(1 - \Phi_H)] \tag{5}$$

for a binary blend as shown in our previous work.[23] The domain spacings calculated by eqs 4 and 5 are shown by the broken lines in Figures 3 and 4, respectively.

On the other hand, if all the homopolymers are distributed uniformly in the corresponding lamella, the lamella will be extended uniformly, so that its thickness should increase as

$$D_i = D_0/[2(1 - \Phi_H)^{1/3}] \tag{6}$$

By using eq 6, the domain spacing for a ternary blend can be derived as

$$D = D_0/(1 - \Phi_H)^{1/3} \tag{7}$$

while it can be written by

$$D = D_0(2 - \Phi_H)/[2(1 - \Phi_H)^{1/3}] \tag{8}$$

for a binary blend. The domain spacings evaluated by eqs 7 and 8 are shown by the dotted lines in Figures 3 and 4, respectively.

**Table 3. Proportion, *x*, of the Homopolymer Localized at the Center of the Corresponding Lamellar Microdomain**

| $M_H/M_B$[a] | ternary blend[b] | binary blend[b] |
|---|---|---|
| 0.05 (0.08) | 0.04 | 0.47 (0.35) |
| 0.17 (0.22) | 0.48 | 0.68 (0.62) |
| 0.38 (0.40) | 0.70 | |
| 0.78 (0.79) | 0.80 | 0.95 (0.93) |

[a] $M_H/M_B$ is the molecular weight ratio of the mixed homopolymer to the corresponding block chain. The numbers in parentheses are those for VPK's. [b] These values for ternary and binary blends were evaluated by the least-squares fits of eqs 10 and 11 to the experimental data shown in Figures 3 and 4, respectively. The numbers in parentheses are the results for the binary blends with VPK's.

It is obvious from these figures that the broken lines are much higher than the dotted lines. Further, it was found that all the experimental data are in between the two calculated curves, i.e., the broken and dotted lines, and they are getting closer to the broken line with increasing $M_H$. These results imply that all the homopolymers in the blends studied in this work must be distributed in microdomains in the intermediate states of the two extreme cases described above. For simplicity, therefore, we assume that the volume fraction of the homopolymers, which are perfectly localized in the middle of the lamella, is $x\Phi_H$ $(0 \le x \le 1)$, and the remaining homopolymers with the volume fraction of $(1 - x)\Phi_H$ are dissolved uniformly in the lamella. Consequently, the thickness of the lamella can be expressed by the sum of contributions from the homopolymers dissolved in the two different manners, i.e., perfect localization and uniform solubilization, as

$$D_i = D_0/[2(1 - \Phi_H)^{1/3}(1 - x\Phi_H)^{2/3}] \tag{9}$$

By using eq 9, the lamellar domain spacing for a ternary blend is derived as

$$D = D_0/[(1 - \Phi_H)^{1/3}(1 - \mathrm{x}\Phi_H)^{2/3}] \tag{10}$$

Similarly, $D$ for a binary blend can be given by

$$D = D_0(2 - \Phi_H)/[2(1 - \Phi_H)^{1/3}(1 - x\Phi_H)^{2/3}] \tag{11}$$

Assuming that $x$ is independent of $\Phi_H$, we evaluated its values by the least-squares fits of eqs 10 and 11 to the experimental data shown in Figures 3 and 4, respectively. The resultant best-fitted curves are shown by the solid lines in these figures, and the evaluated values of $x$ are listed in Table 3. In both ternary and binary blends the proportion of the homopolymers localized at the center of the corresponding lamella is found to increase with increasing $M_H$. This $M_H$ dependence of homopolymer distribution is qualitatively consistent with those reported by Hashimoto et al.,[7] Winey et al.,[13] and Mayes et al.[14] Comparing a ternary and a binary blend at a given $M_H$, we found that the homopolymers in a binary blend are more localized at the center of the lamella than those in a ternary blend. Neutron reflection studies are now in progress to clarify the homopolymer distributions in lamellar microdomains for both ternary and binary blends in more detail.[24]

In ternary blends and binary ones with RMS's, the radii of gyration of PS block chains are not much different from that for a pure diblock copolymer irrespective of $M_H$, at least along the direction parallel to lamellar interface, i.e., $x$-direction. As for the blends except the ternary blends with the homopolymers having $M_H/M_B = 0.05$, this result may be reasonable since most of the blended homopolymers tend to be localized at the center of lamellar microdomain as shown in Table 3. As for the ternary blends with the homopolymers having considerably low $M_H$'s, on the other hand, our SANS result differs from the previous one[16] that block chains are more contracted than pure block polymers along $x$-direction. In the previous work, however, ordinary (not phase-matched) homopolymers were used for preparing contrast-matched blend specimens,[16] so that the scattering intensities observed may not consist only of the single-chain scattering from block chains, but they may be contaminated by intermolecular scattering and also by single-chain scattering from homopolymer chains. If we assume that block chains are extended along the direction perpendicular to lamellar interface, i.e., $y$-direction, at the same degree as that of the extension of lamellar thickness by perfectly uniform solubilization of homopolymers and that they are contracted along the $x$-direction to keep their own volumes constant, $\gamma_x$ can be derived from eq 6 as

$$\gamma_x = (1 - \Phi_H)^{1/6} \tag{12}$$

However, the experimental $\gamma_x$ values for the ternary blends with $M_H/M_B = 0.05$ are higher than from eq 12 shown by the solid line in Figure 6, though the experimental errors are somewhat large. The block chains in such ternary blends may be contracted along the $x$-direction according to eq 12, but this contraction of block chains could be compensated by the expansion due to the excluded volume effects between the segments of a block chain caused by the mixing with homopolymers, as observed for large homopolymers mixed with small ones in melts.[25] Thus, the radii of gyration of block chains along the $x$-direction in such ternary blends are almost the same as that for a pure diblock copolymer.

In binary blends with VPK's, $R_{g,x}$'s of PS block chains are also not much different from that for a pure diblock copolymer irrespective of $M_H$ as well as $\Phi_H$. In the blends with the VPK's having relatively high $M_H$'s, the distances between the nearest chemical junctions, $a_J$, on lamellar interface may be unchanged from that for a pure diblock copolymer since such VPK's are localized at the center of P2VP lamella, so that the thickness of PS lamella, $D_{PS}$, may not be changed by the mixing of VPK's. Thus, the chain conformations of PS block chains in these blends may be unchanged from that for a pure diblock copolymer. In the blends with the VPK's having considerably low $M_H$'s, on the other hand, if the VPK's could be uniformly dissolved in P2VP domain, PS lamella would be extended along the $x$-direction, i.e., $a_J$ would increase, so that the PS lamella would be contracted along the $y$-direction, i.e., $D_{PS}$ would decrease to keep the segment density constant. This speculation is shown by the dotted lines in Figure 4, i.e., eq 8, which exhibit that $D/D_0$ value becomes slightly lower than unity with increasing $\Phi_H$. Although the reduction of $D$ ($=D_{PS} + D_{P2VP}$) was not clearly observed experimentally even for the blends with the VPK having $M_H/M_B = 0.08$ as the VPK's are not uniformly dissolved in the P2VP domain, $D_{PS}$ is expected to be reduced from that of a pure diblock copolymer as reported by Hashimoto et al.[7] If we assume that the chain conformations of the PS block chains in these blends are contracted along the $y$-direction with the reduction of PS lamellar thickness and that they are extended along the $x$-direction to preserve the same degree of coil overlapping as that for a pure diblock copolymer, $\gamma_x$ can be derived from eqs 9 and 11 as

$$\gamma_x = (1 - x\Phi_H)^{1/3}/(1 - \Phi_H)^{1/3} \tag{13}$$

The values of $\gamma_x$, evaluated for the blends with the VPK having $M_H/M_B = 0.08$ using $x$ (0.35) shown in Table 3 are shown by the solid line in Figure 7b, and they are quite consistent with the present data within the experimental errors.

**Acknowledgment.** N.T. acknowledges a partial support of this work by Research Fellowships of the Japan Society for the Promotion of Science for Young Scientists. We express our thanks to Mrs. H. Choshi and T. Watanabe of Nagoya University in preparing poly(styrene-$d_8$-*ran*-styrene-$h_8$)s (RMS). We thank Prof. S. Tsuge, Dr. H. Ohtani, and Y. Ishida of Nagoya University for their advice and cooperation in pyrolysis-gas chromatography-mass spectrometry (PyGC-MS) experiments on determination of the contents of the styrene-$d_8$ segment in RMS's.

## References and Notes

(1) Present address: Mitsubishi Heavy Industries, Ltd., Iwatsuka, Nakamura-ku, Nagoya 453, Japan.
(2) Hong, K. M.; Noolandi, J. *Macromolecules* **1983**, *16*, 1083.
(3) Whitmore, M. D.; Noolandi, J. *Macromolecules* **1985**, *18*, 2486.
(4) Zin, W.-C.; Roe, R.-J. *Macromolecules* **1984**, *17*, 183.
(5) Roe, R.-J.; Zin, W.-C. *Macromolecules* **1984**, *17*, 189.
(6) Tanaka, H.; Hasegawa, H.; Hashimoto, T. *Macromolecules* **1991**, *24*, 240.
(7) Hashimoto, T.; Tanaka, H.; Hasegawa, H. *Macromolecules* **1990**, *23*, 4378.
(8) Winey, K. I.; Thomas, E. L.; Fetters L. J. *J. Chem. Phys.* **1991**, *95*, 9367.
(9) Winey, K. I.; Thomas, E. L.; Fetters L. J. *Macromolecules* **1992**, *25*, 422.
(10) Winey, K. I.; Thomas, E. L.; Fetters L. J. *Macromolecules* **1992**, *25*, 2645.
(11) Koizumi, S.; Hasegawa, H.; Hashimoto, T. *Makromol. Chem., Macromol. Symp.* **1992**, *62*, 75.
(12) Koizumi, S.; Hasegawa, H.; Hashimoto, T. *Macromolecules* **1994**, 27, 6532.
(13) Winey, K. I.; Thomas, E. L.; Fetters, L. J. *Macromolecules* **1991**, *24*, 6182.
(14) Mayes, A. M.; Russell, T. P.; Satija, S. K.; Majkrzak, C. F. *Macromolecules* **1992**, *25*, 6523.
(15) Matsushita, Y.; Torikai, N.; Mogi, Y.; Noda, I.; Han, C. C. *Macromolecules* **1994**, *27*, 4566.
(16) Hasegawa, H.; Tanaka, H.; Hashimoto, T.; Han, C. C. *J. Appl. Crystallogr.* **1991**, *24*, 672.
(17) Quan, X.; Koberstein, J. T. *J. Polym. Sci. Part B, Polym. Phys.* **1987**, *25*, 1381.
(18) Matsushita, Y.; Nakao, Y.; Saguchi, R.; Choshi, H.; Nagasawa, M. *Polym. J.* **1986**, *18*, 493.
(19) There is no essential difference between SP-77 and SP-43. SP-43 was additionally prepared to make blends with DP-77 because SP-77 has been consumed completely in the middle of experiments in this study.
(20) Matsushita, Y.; Mori, K.; Saguchi, R.; Nakao, Y.; Noda, I.; Nagasawa, M. *Macromolecules* **1990**, *23*, 4313.
(21) Matsushita, Y.; Nakao, Y.; Saguchi, R.; Mori, K.; Choshi, H.; Muroga, Y.; Noda, I.; Nagasawa, M.; Chang, T.; Glinka, C. J.; Han, C. C. *Macromolecules* **1988**, *21*, 1802.
(22) Matsushita, Y.; Mori, K.; Mogi, Y.; Saguchi, R.; Noda, I.; Nagasawa, M.; Chang, T.; Glinka, C. J.; Han, C. C. *Macromolecules* **1990**, *23*, 4317.
(23) Matsushita, Y.; Torikai, N.; Mogi, Y.; Noda, I.; Han, C. C. *Macromolecules* **1993**, *26*, 6346.
(24) Torikai, N.; Matsushita, Y.; Noda, I.; Karim, A.; Satija, S. K.; Han, C. C., to be published.
(25) Matsushita, Y.; Takabayashi, N.; Torikai, N.; Noda, I., in preparation.

MA961936O